Analysis of Velocity Measurements about a Hemisphere-Cylinder Using a Laser Velocimeter

Tsuying Hsieh*
ARO Inc., Arnold Engineering Development Center, Arnold Air Force Station, Tenn.

For velocity measurements using a laser velocimeter, the primary concern is particle lag. The influence of particle size, particle density, and model dimensions about a hemisphere-cylinder in the Mach number range from 0.85 to 1.3 is investigated. It is found that particle lag can be reduced by decreasing the size and density of tracer particles or by increasing the relative model dimensions. Hence, model-scale effect generally is presented in data measured by a laser velocimeter. The concept of using an effective particle to represent the spectrum of tracer particles in a flow environment has been evaluated and found to be useful. When the particle lag is taken into account, the theoretical velocity field for a hemisphere-cylinder agrees well with experimental data.

Nomenclature

C_D = drag coefficient
f = factor for drag coefficient, Eq. (2b)
G = ratio of ρ_p and ρ_∞
K_p = particle Knudsen number, $\lambda/2r_p$
L = model characteristic length
M = flow Mach number
M_p = particle Mach number, $|w-w_p|M/\sqrt{T}$
R = radius of hemisphere-cylinder
R_L = model Reynolds number, $2LU_\infty/\nu$
Re_p = particle Reynolds number, Eq. (2c)
r_p = particle radius
T = temperature of the gas, nondimensionalized by T_∞
T_∞ = freestream temperature
t = time, nondimensionalized by L/U_∞
U,V = axial and radial velocity components, respectively, nondimensionalized by U_∞
w = velocity vector, nondimensionalized by U_∞
U_∞ = freestream velocity
Y,Z = radial and axial coordinates, nondimensionalized by L
α = ratio of r_p and L
λ = mean free path of the gas
ν = kinematic viscosity of the gas
ρ = density of the gas, nondimensionalized by ρ_∞
ρ_p = particle density, nondimensionalized by ρ_∞
ρ_∞ = freestream density

Subscripts

p = particle
s = shock
∞ = freestream

Introduction

THE use of laser velocimeters (LV) for velocity measurements in fundamental or engineering investigations of flow problems is increasing. Since the LV measures the velocity of tracer particles entrained in the fluid medium rather than the velocity of the fluid itself, there is primary concern about how well the particle follows the true fluid velocity (so-called particle lag). For wind-tunnel applications, particularly in the presence of a shock, particle lag can be a serious problem. Many investigators[1-3] have made calculations of the motion of a small particle in a flowfield for the purpose of analyzing data obtained by LV; however, such theoretical computations always are impaired by unknown particle properties, such as size and density. A direct determination of particle properties for an unseeded wind tunnel is difficult, if not impossible, and seeding with sufficiently small particles for a large wind-tunnel application is impractical. Therefore, a means of representing the tracer particles is desired to understand the LV data better. First, this paper presents an analysis for the mean motion of a small particle in a given flowfield by emphasizing the important parameters that govern the particle motion and the significance of these parameters in relation to the data. Second, in order to represent the spectrum of tracer particles contained in a flow environment such as a wind tunnel, the concept of an effective particle size and density is investigated. Experimental LV measurements and theoretical velocity field computations have been made for flow past a hemisphere-cylinder in the low supersonic and transonic Mach number range. The analysis presented also can serve as a guide to indicate the kind of particles that are needed in the flow medium for a specified tolerance of particle lag.

Received Aug. 2, 1976; revision received Nov. 29, 1976.
Index categories: Subsonic and Transonic Flow; Supersonic and Hypersonic Flow; Lasers.
*Research Engineer. Member AIAA.

Analysis

For LV application, the nondimensional equation of motion for a particle traveling in the gas flowfield is given by[4]

$$\frac{dw_p}{dt} = \frac{3}{8}\cdot\frac{C_D}{\alpha G}\rho\,|w-w_p|\,(w-w_p) \qquad (1)$$

It is seen that particle motion is characterized by three parameters: the ratio of particle radius to a characteristic length α, the ratio of particle density to the freestream gas density G and the drag coefficient of the particle C_D. The significance of α and G in LV applications may be described as follows.

The Ratio α

The value of α can be varied in two ways: by varying r_p while holding L constant, or by varying L while holding r_p constant. The former approach (varying r_p) has been used by many investigators[1-3] in LV applications to indicate the effect of particle size. However, the effect of varying L rarely has been mentioned. If the size distribution of tracer particles for given flow environment is constant, different particle velocities would be expected for different-sized models. Similarly, different measured results would be expected for the same model tested with different sizes of tracer particles. This is the so-called scale effect (discussed later). It is well known that particle lag can be reduced by using smaller

particles. Since there is a limit to the reduction of particle size that can be provided in the flow medium, the alternate way to achieve the same goal would be to increase the model size.

The Ratio G

The ratio G indicates the importance of particle inertia. The larger the G value is, the greater will be the particle lag when subject to a velocity gradient of the fluid medium. Therefore, it is desirable to have tracer particles with a low G value.

The drag coefficient C_D also plays an important role in Eq. (1). In general, C_D depends on the particle Reynolds number, Mach number, and Knudsen number, if the particle becomes sufficiently small ($2r_p \lesssim 0.1\ \mu$, say). The dependence of C_D on Re_p and M_p for spheres has been studied,[5,6] and a convenient, functional form for C_D in terms of K_p in the Stokes flow regime has been reported.[7] In the present study, however, the flow region for the spherical particle is within the continuum region ($K_p \approx 0.05 << 1$), and M_p value always is less than 0.4; thus, the dependence of C_D on M_p and K_p can be neglected.[5,7] Also, in the present study $Re_p \lesssim 100$; thus, the following expression for C_D accurately represents the experimental data for spheres.[8]

$$C_D = (24/Re_p) f(Re_p) \tag{2a}$$

$$f = 1 + 0.197\, Re_p^{0.63} + 2.6\times 10^{-4} Re_0^{1.38} \tag{2b}$$

$$Re_p = R_L \rho \alpha\, |w - w_p| \tag{2c}$$

The calculation of inviscid flow over a hemisphere-cylinder in the low supersonic and transonic Mach number range has been reported.[9] Two techniques were used in the calculation for $M_\infty > 1$: 1) a time-dependent solution to the Euler equations with shock fitting, and 2) a relaxation solution to the full potential equation with smeared shock.[10] Method 2 also can compute for $M_\infty < 1$. Therefore, the gas velocity field for a hemisphere-cylinder[9] is used in this study for $M_\infty = 0.85$, 1.1, 1.2, and 1.3. The coupled equations for particle motion over a hemisphere-cylinder can be written as follows:

$$\frac{\partial Z_p}{\partial t} = U_p \tag{3a}$$

$$\frac{\partial U_p}{\partial t} = \frac{9}{R_L}\frac{fu}{G\alpha^2}(U - U_p) \tag{3b}$$

$$\frac{\partial Y_p}{\partial t} = V_p \tag{3c}$$

$$\frac{\partial V_p}{\partial t} = \frac{9}{R_L}\frac{fv}{G\alpha^2}(V - V_p) \tag{3d}$$

where

$$fu = f|U - U_p| / |w - w_p|$$

$$fv = f|V - V_p| / |w - w_p|$$

$$|w - w_p| = [(U - U_p)^2 + (V - V_p)^2]^{1/2}$$

To specify the initial conditions, it is assumed that the particle velocity is in equilibrium with the freestream gas velocity up to the shock point in method 1 and is not affected by the presence of a shock. Then,

$$Z_p = Z_s \quad Y_p = Y_s \quad U_p = 1 \quad V_p = 0 \quad (t \le 0) \tag{4a}$$

For method 2, the initial condition is set at $Z/R = -4$, or

$$Z_p = -4 \quad Y_p = Y \quad U_p = 1 \quad V_p = 0 \quad (t \le 0) \tag{4b}$$

The particle trajectory and velocity components can be computed by integrating Eqs. (3) and (4). A fourth-order Runge-Kutta method is used in the integration. (The computer program is available upon request.)

Experiments

LV measurements of axial and radial velocity components for flow past a hemisphere-cylinder were performed in the Arnold Engineering Development Center (AEDC) aerodynamic wind tunnel (IT) at $M_\infty = 1.3$, 1.2, 1.1, and 0.85. The wind tunnel is a continuous-flow, nonreturn type. The hemisphere-cylinder was 2.54 cm diam and 25.4 cm long and was sting-mounted. The LV used for the measurements is a two-component, dual-scatter, Bragg cell type of system operating in the on-axis backscatter collection mode with a 1.5-W argon ion laser. The system is capable of measuring velocity in the range from -152 to 490 m/sec for the axial component and ± 122 m/sec for the radial component. The entire optical system is mounted on a three-axis translating mechanism, with a position resolution accuracy of ± 0.0025 cm in all three directions. The scattering source (or tracer particle) is the natural aerosol particles entrained in the flow medium. In order to obtain a sound statistical sample, about 1000 samples were taken in each measurement. Details of the experimental facilities and LV system can be found in Refs. 1 and 2 and references therein.

Results and Discussion

Analytical Study of Influence of Tracer Particle and Model Scale

The influence of tracer particles may be investigated analytically by varying ρ_p and r_p, and the influence of model scale may be investigated by varying $L(=R)$. Oil drops, water drops, and dust with density varying from 0.4 to 2.4 g/cm^3 are most likely to be entrained in common flow environment. To study the influence of ρ_p, r_p, and R, a typical particle of $\rho_g = 0.8$ g/cm^3 and $r_p = 5.2\ \mu$ is used as a reference particle, and a hemisphere-cylinder of $L = R = 1.27$ cm is used as a reference model size. The computed particle velocity along the axis between the bow shock and the nosetip of the hemisphere-cylinder is given for $M_\infty = 1.2$ on Fig. 1. The broken curve is the theoretical gas velocity obtained by method 1.[9] Curve 1 represents the reference case; it is seen that the particle lag is significant. The model size is varied first. For curve 2, the size of the model is increased by 10 times, and significant reduction in particle lag is obtained. Curve 2 also demonstrates the scale effect, as mentioned earlier. For curve 3, the particle size is decreased by 5.2 times from the reference particle, with other conditions kept constant. It is interesting to notice that the particle lag is not as great as that shown by curve 2. Finally, the particle density alone is reduced by five times, as shown by curve 4. The particle lag also is improved but is not as significant as in curve 3. Thus, the influence of r_p is more pronounced than ρ_p and L.

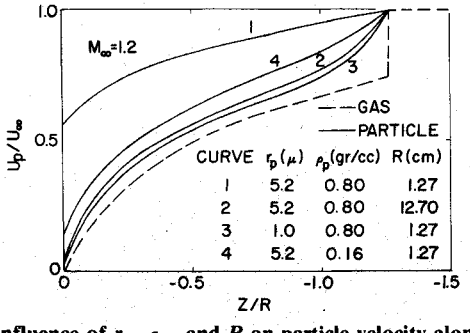

Fig. 1 Influence of r_p, ρ_p, and R on particle velocity along axis of hemisphere-cylinder.

Effective Particle Size for Experiment

In a flow environment, the size and density distribution of tracer particles can be very broad, and they are difficult, if not impossible, to measure. In each LV sampling, the velocity is represented by statistical mean value of the sampled particles; therefore, the individual particle behavior is not important, but the collective, or representative, particle is of practical meaning. Thus, an effective particle can be used to represent the average tracer particles entrained in the flow medium.

In Fig. 2, the velocity along the axis of a hemisphere-cylinder is shown for $M_\infty = 1.1$, 1.2, and 1.3. The solid and chain curves are the theoretical gas velocity computed with methods 1 and 2, respectively. Method 2 does not give a sharp location of the shock, as expected; however, the agreement of the two methods downstream of the shock is excellent. The experimental data measured by LV (mean value of all samples) also are plotted in Fig. 2. It is seen that the shock location predicted by method 1 is indeed in good agreement with the LV measurements. (The theory also agrees well with shadowgraphs.[9]) The particle lag for the velocity field behind the shock under investigation is shown by the difference between the solid or chain curves and the experimental data. Now, if the spectrum of tracer particles in the wind tunnel can be represented by an effective particle, a set of ρ_p and r_p values which would fit all three sets of data as shown in Fig. 2 should be achievable. This idea proves to be valid, as shown in Fig. 2 by the computed U_p data for particles with $\rho_p = 0.8$ g/cm^3 and $r_p = 1.37$ μ (ρ_p value is chosen first, and r_p is determined by trial and error), where dashed and double-dot-chain curves correspond to U_p as computed from U obtained by methods 1 and 2, respectively. (Note that $R = 1.27$ cm throughout the rest of the paper.) Obviously, there can be other combinations of ρ_p and r_p which will fit the same sets of data. It has been found that $\rho_p = 0.4$, $r_p = 2.0$; $\rho_p = 1.2$, $r_p = 1.07$; and $\rho_p = 2.4$ g/cm^3, $r_p = 0.7$ μ also can fit the data well. Operation of the AEDC aerodynamic wind tunnel results in steam being exhausted in the vicinity of the air intake. Therefore, it is felt that $\rho = 0.8$ g/cm^3 is a reasonable value to simulate the tracer particle density in this experiment; hence, from this point on the effective particle is represented by $\rho_p = 0.8$ g/cm^3 and $r_p = 1.37$ μ.

Comparison of LV Data with Theory for a Hemisphere-Cylinder

A comparison of measured and computed particle velocity is shown in Fig. 3 for $M_\infty = 1.2$ at $Y/R = 2$, 3, and 4 in the nose portion and along the radial direction at the juncture of hemisphere and cylinder ($Z/R = 1$) for $M_\infty = 1.1$ and 1.2. The purpose is threefold: first, to compare between methods 1 and 2; second, to compare between theory and experiment; and third, to compare the experiment with the computed U_p, V_p for the effective particle. From Fig. 3, it is seen that the comparison between methods 1 and 2 is generally good within the shock layer. The data compare much better with the U_p and V_p as computed for the effective particle. This implies that the difference between theoretical flow and experimental particle velocity is due to particle lag. This is particularly clear

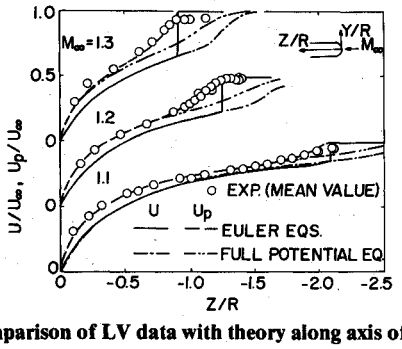

Fig. 2 Comparison of LV data with theory along axis of hemisphere-cylinder.

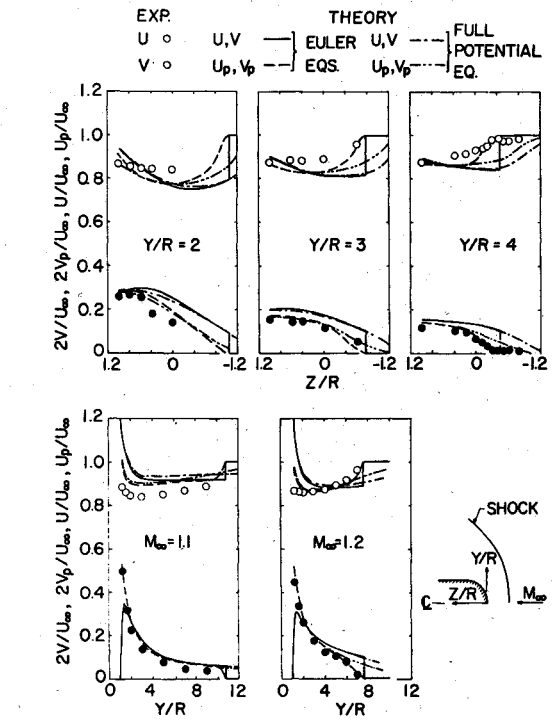

Fig. 3 Comparison of U and V components of LV data with theory at the nose portion of hemisphere-cylinder.

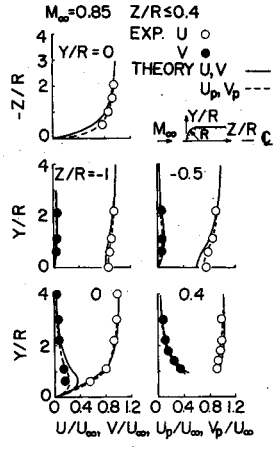

Fig. 4 Comparison of U and V components of LV data with theory for hemisphere-cylinder.

in the situation for the radial component near the hemisphere-cylinder surface in Fig. 3, where the inviscid theory requires $V \to 0$, whereas the particle dynamics with effective particle predict correct vertical component. The comparison of axial components near the surface is not satisfactory in Fig. 3, perhaps because of the viscous effect. (For $M_\infty = 1.1$, the data are consistently lower.)

Applications

For an unseeded flow environment, the procedure described in this paper may be used as a means to obtain the effective particle or as a means of tracer particle calibration. With the help of effective particles, the particle lag can be evaluated accurately. For example, the same effective particle is applied to the case of flow past a hemisphere-cylinder at $M_\infty = 0.85$ where no bow shock is present for $Z/R \leq 0.4$. (Flow separates at $Z/R = 0.7$; hence, inviscid theory for gas velocity is not valid in this case. However, inviscid solution is considered to be valid for $Z/R \leq 0.4$.[11]) As shown in Fig. 4, the agreement between U_p and V_p and the experimental data is excellent.

The present analysis can help the experimentalist to determine what size and density of tracer particles are required in order to satisfy a specified tolerance of accuracy in

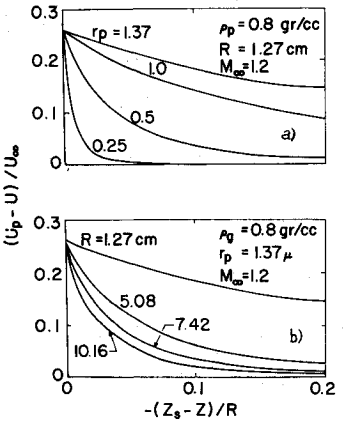

Fig. 5 Particle lag vs distance behind shock as a function of a) r_p and b) R along axis of hemisphere-cylinder.

velocity measurements for a given model scale, or vice versa. For example, Fig. 5a shows the particle lag along the axis behind the shock for a hemisphere-cylinder ($R = 1.27$ cm) at $M_\infty = 1.2$ for $\rho_p = 0.8$ g/cm^3 and $r_p = 1.37$, 1, 0.5, and 0.25 μ. Thus, if the particle lag is allowed to occur only within $(Z_s - Z) = 0.1R$ behind the shock with 3% allowable error in velocity measurements, $r_p = 0.5$ μ is sufficient; if $Z_s - Z = 0.02R$ is required, then $r_p = 0.25$ is necessary. On the other hand, if the tracer particles are natural aerosol, as in the present experiment with $r_p = 1.37$ μ, then the required model radius R would be approximately 7.42 cm in order to keep particle lag to within $(Z_s - Z) = 0.1R$, as shown in Fig. 5b.

Conclusions

1) The particle lag in a given flowfield is determined by the particle radius, particle density, and model size. The particle lag can be reduced by decreasing the radius or density of the tracer particle or by increasing the size of the model. The influence of particle radius on particle lag is more pronounced than the influence of either particle density or model size.

2) It is important to realize that a model-scale effect generally is present in velocity measurements using a laser velocimenter unless the particle lag is everywhere negligibly small.

3) The average property of tracer particles for a given flow environment may be represented by an effective particle. A procedure is described to determine the effective particle.

4) The time-dependent solution to Euler equations with shock fitting can predict the velocity field for flow past a hemisphere-cylinder at low supersonic Mach numbers. The predicted shock location agrees with laser velocimeter measurements. The velocity field predicted by the relaxation solution to the full potential equation without shock fitting agrees well with the solution to the Euler equations within the shock layer for Mach numbers of 1.1, 1.2, and 1.3. At a Mach number of 0.85, the solution to the full potential equation can predict the velocity field satisfactorily over a hemisphere-cylinder before the flow separates.

Acknowledgment

The research reported herein was conducted by the Arnold Engineering Development Center (AEDC), Air Force Systems Command (AFSC). Results were obtained by personnel of ARO, Inc., Contract Operator at AEDC. The author wishes to thank C. F. Lo for helpful discussions, V. Cline for taking the LV data, and G. Lewis for computing the results.

References

[1]Yanta, W. J., "Turbulence Measurements with a Laser Doppler Velocimeter," Naval Ordnance Lab., White Oak, Md., NOLTR 73-94, May 1973 (and references therein).

[2]Maxwell, B. R., "Tracer Particle Flow in a Compressor Rotor Passage with Application to LDV," *AIAA Journal*, Vol. 13, Sept. 1975, pp. 1141-1142.

[3]Putnam, L. E. and Meyer, J. V., "Measurements of Flow Fields in a Large Transonic Wind Tunnel Using a Laser Velocimeter," AIAA Paper 1425, General Aviation Technologyfest, Wichita, Kansas, Nov. 13-14, 1975.

[4]Soo, S. L., *Fluid Dynamics of Multiphase System*, Blaisdell Publishing Co., Waltham, Mass., 1967.

[5]Bailey, A. B. and Hiatt, J., "Free-Flight Measurements of Sphere Drag at Subsonic, Transonic, Supersonic, and Hypersonic Speeds for Continuum, Transition, and Near-Free-Molecular Flow Conditions," Arnold Engineering Development Center, Arnold Air Force Station, Tenn., AEDC-TR-70-291, March 1971.

[6]Walsh, M. J., "Influence of Drag Coefficient Equations on Particle Motion Calculations," *Proceedings of Minnesota Symposium on Laser Anemometry*, Univ. of Minn., Oct. 22-24, 1975.

[7]Phillips, W. F., "Drag on a Small Sphere Moving Through a Gas," *The Physics of Fluids*, Vol. 18, Nov. 9, 1975, pp. 1089-1093.

[8]Langmuir, I. and Blodgett, K. B., "A Mathematical Investigation of Water Droplet Trajectories," Army Air Forces TR 5418, Feb. 1946.

[9]Hsieh, T., "Hemisphere-Cylinder in Low Supersonic Flow," *AIAA Journal*, Vol. 13, Dec. 1975, pp. 1551-1552.

[10]South, J., Jr. and Jameson, A., "Relaxation Solutions for Inviscid Axisymmetric Transonic Flow Over Blunt or Pointed Bodies," *Proceedings of AIAA Computational Fluid Dynamics Conference*, July 16-18, 1973.

[11]Hsieh, T., "An Investigation of Separated Flow About a Hemisphere-Cylinder at 0 to 19 deg Incidence in the Mach Number Range from 0.6 to 1.5," Arnold Engineering Development Center, AEDC-TR-76-112, July 1976; also AIAA Paper 77-179, Jan. 1977.

[12]Lo, C. F., "Transonic Flow Field Measurements Using a Laser Velocimeter," *Proceedings of Minnesota Symposium on Laser Anemometry*, Univ. of Minnesota, Oct. 22-24, 1975, pp. 112-123.